Low-Temperature Thermal Expansion of Zinc Oxide. Vibrations in Zinc Oxide and Sphalerite Zinc Sulfide

B. Yates* and R. F. Cooper†
Department of Pure and Applied Physics, University of Salford, Salford M5, 4WT, *Lancaster, United Kingdom*
and
M. M. Kreitman*
Department of Physics, University of Dayton, Dayton, Ohio 45409
(Received 31 December 1970)

New measurements of the linear thermal-expansion coefficients $\alpha_{\parallel}$ and $\alpha_{\perp}$ in the c and a crystallographic axis directions of ZnO are reported between 90 and 260 °K. Grüneisen parameters $\gamma_{\parallel}$ and $\gamma_{\perp}$, defined for strain coordinates parallel and perpendicular to the c axis, respectively, have been calculated from the present thermal-expansion coefficients and related data. Similar calculations have been performed for ZnS, with modifications appropriate to cubic symmetry, using earlier experimental results for specific heat, thermal expansion, and elastic constants. The Grüneisen parameters fall from positive values at room temperature to negative values at low temperatures, and in the case of zinc oxide, interpolation has been employed to obtain the mean low-temperature limiting value of γ_0 calculated from the pressure dependence of the elastic constants. A quasiharmonic approximation has been applied to calculate the characteristic temperatures $\theta(n)$ corresponding to the maximum frequencies $\omega_D(n)$ of the Debye distributions having the same nth moments $\langle\omega^n\rangle$ as the specimens for $-3 \leq n \leq 6$. In the case of zinc oxide, the similarity of the dimensional dependences of the moments, defined by $\gamma(n) = \sum\gamma_j\omega_j^n / \sum\omega_j^n$ corresponding to $\gamma_{\parallel}(n)$ and $\gamma_{\perp}(n)$, indicates a low degree of crystal anisotropy, while their variations with n suggest that transverse modes of vibration predominate among the low-frequency modes, and longitudinal modes predominate among the high-frequency modes. The account concludes with calculations of the rms displacements of the atoms in both compounds considered as functions of temperature between 0 and 300 °K.

I. INTRODUCTION

The II-VI compounds have aroused a good deal of interest over the past few years for a variety of reasons, a measure of which has been provided by summaries of the volume of work performed.[1,2] In order to analyze the vibrations in these compounds and to analyze properties of the vibrational frequency spectra, knowledge of the specific heat, thermal expansion, and elastic constants are required, ideally over a wide range of low temperatures. An examination of the available thermodynamic data for the oxides, sulfides, selenides, and tellurides of zinc, cadmium, and mercury revealed the existence of a large number of gaps. Indeed, it was only for zinc oxide and zinc sulfide that sufficiently complete sets of data existed to justify thermodynamic analysis, and even in these cases the analyses could only be embarked upon with reservations. These two solids are particularly interesting from an analytical point of view, since zinc oxide possesses hexagonal symmetry, whereas the symmetry of sphalerite zinc sulfide is cubic.

Comprehensive reviews of the extensive investigations of the optical properties of II-VI compounds have been given,[3] and manifestations of piezoelectric and pyroelectric effects in zinc oxide, which are also displayed by other compounds having the wurtzite structure, have been studied.[4] Meanwhile Damen *et al.*[5] have determined the frequency and symmetry character of the fundamental Raman-active modes from a polarization study of the 90° scattering. Earlier, samples of zinc oxide had been discovered[6] which possessed abnormally high electrical conductivities and abnormally high- and positive-temperature coefficients of electrical conductivity. Correlation between the incidence of these anomalies and exposure to damp conditions was observed, and it was possible to associate the changes in electrical properties and changes in axial ratio with lattice distortions which, it was considered, might be associated with contamination of this type. Apart from interest in the thermal and elastic properties of zinc oxide, which will be summarized later, mention may be made at this point of the work of Chung and Buessem,[7] who showed that the Voigt-Reuss-Hill approximation, from which the polycrystalline elastic constants might be calculated in terms of the anisotropic single-crystal elastic constants, was accurately applicable to zinc oxide.

Turning to zinc sulfide, the dispersion relations, frequency-distribution function, and specific heat have been calculated[8] on the basis of a model containing short-range and long-range Coulombic interactions. Czyzak *et al.*[9] made etch-pit and x-

ray studies of zinc sulfide, from which they confirmed that stacking disorders commonly accompanied both the zinc blende (sphalerite) and wurtzite modifications of this compound, and Majumdar and Roy[10] drew attention to the occurrence of polymorphism in zinc sulfide during the course of their investigation of the p-T dependence of the sphalerite-wurtzite transition. In fact many structures are possible between the cubic and hexagonal close-packed limiting cases. Keyes[11] reduced the elastic moduli and characteristic lattice vibrational frequencies of semiconductors having the diamond, zinc-blende, and wurtzite structures to dimensionless parameters, using reststrahl frequencies. He found that a classification of these quantities into divisions defined by compounds formed between particular groups produced rationalizations characterized by relatively small percentage variations with the classes. More recently, the Debye-Waller factors of a number of II-VI compounds have been calculated[12] as functions of temperature, with the aid of breathing shell models. In agreement with an earlier conclusion of Blackman,[13] it has been concluded that the mean square vibrational amplitudes of the two atoms in each of the substances were approximately equal, a result which will prove to be useful when calculating these quantities from the result of an application of the quasiharmonic approximation to experimental thermodynamic results for these solids.

The extent of the existence of calorimetric, thermal-expansion, and elastic-constant data for zinc oxide and zinc blende will be summarized under accounts of the individual compounds. Meanwhile, it will suffice to note that the absence of precise values for the linear coefficients of thermal expansion of zinc oxide below room temperature led the authors to undertake measurements of this quantity, in order to augment existing experimental data and to facilitate the analyses.

II. EXPERIMENTAL DETAILS AND RESULTS

The single-crystal specimens of zinc oxide used in the experimental investigation were available in the form of small rectangular blocks. These were fashioned to the form of small pyramids, each standing on three feet, and were aligned to within half a degree by taking back-reflection Laue photographs. The same set of three specimens was used for measurements parallel to the a and c crystallographic axes. The linear coefficients of thermal expansion of these specimens were measured using interferometric apparatus[14] which has since been modified to give greater sensitivity by the incorporation of a laser in place of the conventional source of illumination and by improved temperature control.[15] Because of problems encountered with rotations of fringes and changes in average fringe spacing, which result from instabilities inherent in this type of system,[16] recourse was made to hollow cylindrical specimens whenever possible in the work of Bailey and Yates[17] and that mentioned earlier. This was not possible in this instance because of a lack of crystal availability. Friction between the optical flats and the specimens, which together made up the interferometer, was very low and no problems were encountered with mechanical instabilities. The specimens were kindly supplied by the Aerospace Research Laboratories, Wright-Patterson Air Force Base, Ohio. The impurity level in the crystals was believed to be at the level of a few parts per million.

The present measurements displayed an average scatter of a little under 3% over the entire temperature range, and they are believed to be accurate in an absolute sense to within 3% at 200 °K, diminishing to 6% at 110 °K. After the initiation of this investigation the results of Ibach[18] appeared, which covered the temperature range 9–800 °K. From Figs. 1 and 2 it will be seen that the maximum disagreement between the two sets of results amounts to approximately 10% at 270 °K in the case of measurements in the a crystallographic-axis direction. At 200 °K and below, agreement between the two sets of results in this direction is excellent, and the same may be said of the agreement between results measured in the c crystallographic-axis direction over the whole temperature range of the present investigation, i.e., 80–270 °K. Because of this agreement the cost of extending the present measurements to lower temperature did not seem to be justified and these were therefore terminated at 80 °K. Agreement with the results of calculations

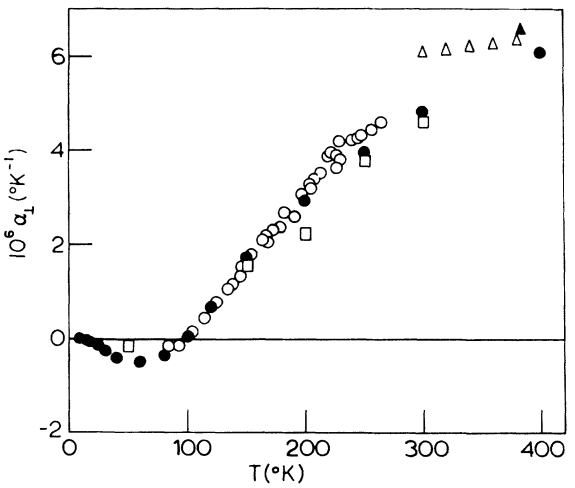

FIG. 1. Linear thermal-expansion coefficient $\alpha_\perp$ of zinc oxide, measured in the "a-a" crystallographic plane, as a function of temperature: ○, present results; ●, Ibach (Ref. 18); □, Reeber (Ref. 21); △, Khan (Ref. 19); ▲, Sirdeshmukh and Deshpande (Ref. 20).

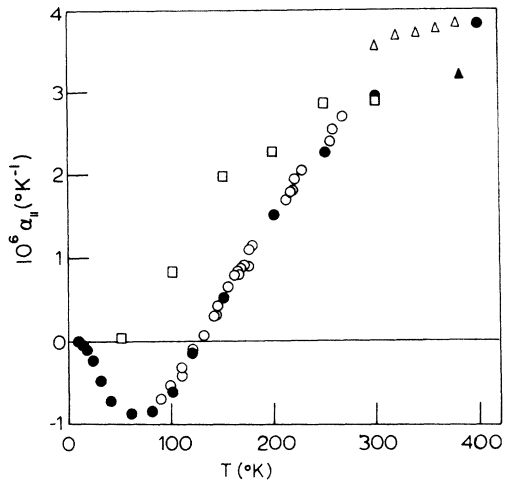

FIG. 2. Linear thermal-expansion coefficient $\alpha_{\parallel}$ of zinc oxide, measured in the c crystallographic-axis direction, as a function of temperature: ○, present results; ●, Ibach (Ref. 18); □, Reeber (Ref. 21); △, Khan (Ref. 19); ▲, Sirdeshmukh and Deshpande (Ref. 20).

based upon x-ray measurements[21] over common ranges of low temperature is not very good in the case of measurements made in the a-axis direction, and in the c direction it is particularly bad. At the higher temperatures a smooth join up with results available from other sources is not observed, and no explanation of these serious discontinuities can be given. The results of the present investigation are summarized in Table I.

III. DISCUSSION

A. Grüneisen Parameter

The volume dependences of the frequencies of lattice vibrations are frequently described in terms of the Grüneisen parameter. The appropriate form of this parameter associated with the ith mode of the lattice vibrations may be expressed as

$$\gamma_i = -\frac{V}{\nu_i}\left(\frac{\partial \nu_i}{\partial V}\right)_T ,$$

in which ν_i is the frequency of the ith normal mode and V is the volume of the crystal. It is necessary to sum these values of γ_i over the whole spectrum, and this is done by taking the weight of each normal mode as its contribution to C_v. Thus, in general, we may write

$$\gamma = \textstyle\sum_i \gamma_i C_{v_i}/C_v ,$$

and the relationship to physically measurably quantities $\gamma = \beta V/(C_p \chi_s)$ is well known, in which β is the volume coefficient of thermal expansion, C_p is the heat capacity of volume V of the solid at constant pressure, and χ_s is the adiabatic compressibility. This is perfectly adequate when dealing with cubic solids, but in the case of anisotropic solids Barron and Munn[22] have shown that more meaning may be derived from the more general equations

$$\gamma_\lambda = \frac{V}{C_\eta}\sum_{\mu=1}^{6}\alpha_\mu c^T_{\mu\lambda} = \frac{V}{C_t}\sum_{\mu=1}^{6}\alpha_\mu c^S_{\mu\lambda} ,$$

in which C_t and C_η are the heat capacities of volume V at constant stress and constant strain, respectively; α_μ are the coefficients of thermal expansion corresponding to the strain coordinates η_μ; $c^T_{\mu\lambda}$ and $c^S_{\mu\lambda}$ are the isothermal and adiabatic elastic constants. In this notation the expression for γ_λ reduces to

$$\gamma_{\parallel} = \frac{V}{C_t}\left(2c^S_{13}\alpha_{\perp} + c^S_{33}\alpha_{\parallel}\right) \tag{1}$$

and

$$\gamma_{\perp} = \frac{V}{C_t}\left[(c^S_{11} + c^S_{12})\alpha_{\perp} + c^S_{13}\alpha_{\parallel}\right] \tag{2}$$

in the case of hexagonal crystals, in which the c^S_{ij} are adiabatic elastic constants and the symbols $\parallel$ and $\perp$ denote directions parallel and perpendicular to the c crystallographic axis, respectively.

1. *Zinc Oxide*

Commonly known as zincite, the structure of zinc oxide resembles that of wurtzite. The zinc atoms are nearly in the position of hexagonal close packing. Every oxygen atom lies within a tetrahedral group of four zinc atoms, and these tetrahedra all point in the same direction along the hexagonal axis, giving the crystal its polar symmetry.

In the analysis which follows, a room-temperature density of 5.606 g cm^{-3} was assumed, leading to $V_{300} = 14.5_1 \pm 0.1_7$ cm^3 mole^{-1}. For the spe-

TABLE I. Linear coefficients of thermal expansion of zinc oxide: $\alpha_{\parallel}$ parallel to the c axis, $\alpha_{\perp}$ perpendicular to the c axis. The α values are given in units of 10^{-6} °K^{-1}.

T(°K)	Present data $\alpha_{\parallel}$	Ibach's data[a] $\alpha_{\parallel}$	Present data $\alpha_{\perp}$	Ibach's data[a] $\alpha_{\perp}$
90	-0.7_0		-0.2_0	
100	-0.5_5	−0.62	0.0_0	0.04
110	-0.3_7		$+0.2_7$	
120	-0.1_6	−0.16	0.5_9	0.64
130	$+0.0_6$		0.9_2	
140	0.2_9		1.2_4	
150	0.5_1	0.50	1.5_6	1.69
160	0.7_4		1.8_9	
170	0.9_5		2.2_1	
180	1.1_5		2.5_3	
190	1.3_4		2.8_5	
200	1.5_1	1.51	3.1_5	2.88
210	1.7_0		3.4_6	
220	1.8_8		3.7_8	
230	2.0_6		4.0_5	
240	2.2_4		4.2_5	
250	2.4_0	2.25	4.4_0	3.90
260	2.5_6		4.5_0	

[a]Reference 18.

cific heat, the available results in the temperature range required consist of those of Maier *et al.*[23] between 88 and 295 °K, and those of Clusius and Harteck[24] between 30 and 200 °K. A compromise was adopted in drawing a smooth curve between these two sets of results, which differed by amounts up to 10% in the regions of overlap. No specific-heat results were available at temperatures below 30 °K. The thermal-expansion data available for zinc oxide have already been summarized. With the exception of the results of some measurements[25] of the fractional variation of c_{33} in the temperature range 25–100 °K, the only elastic-constant data currently available for zinc oxide appear to be those of Bateman,[26] who operated at frequencies between 60 and 500 Mc/sec on two single crystals of high-purity zinc oxide at room temperature. Because of the conjecture which would have been involved in utilizing Tarnow's data, it was decided to take no account of any temperature variation of the elastic constants below room temperature at this stage.

Subject to the limitations imposed by the availability and uncertainty of experimental data, as outlined above, the Grüneisen parameters $\gamma_{\parallel}$ and $\gamma_{\perp}$ were calculated as functions of temperature, producing the results displayed graphically in Fig. 3. Excluding any influence from the temperature variation of the elastic constants, the absolute uncertainties in these values amounts to approximately 20% in the cases of both $\gamma_{\parallel}$ and $\gamma_{\perp}$ at room temperature. Because of the probable uncertainty in the heat-capacity data at the lowest temperatures, values of γ based upon these have not been plotted below approximately 50 °K. Two points are worthy of note at this juncture: (i) $\gamma_{\parallel}$ and $\gamma_{\perp}$ are very similar, implying that the anisotropy of the crystal must be comparatively small, and (ii) $\gamma_{\parallel}$ and $\gamma_{\perp}$ both become negative at low temperatures, suggesting the predominance of transverse modes of vibration at low temperatures. Soga and Anderson[27] have measured the elastic constants of polycrystalline zinc oxide and their dependence upon temperature and pressure, using ultrasonic methods. They found that the pressure dependence of the shear velocity was negative, and on the basis of a method outlined earlier,[28,29] they calculated the Grüneisen parameter at very high and very low temperatures. Good agreement between the very low-temperature value so calculated and that which would be given by experimental specific-heat, thermal-expansion, and elastic-constant data is to be expected, for the acoustic modes of vibration would be expected to predominate at very low temperatures, and significant variations with temperature of the pressure dependences of the elastic constants are not expected. Their "isotropic" value of $\gamma_0 = -1.132$ led them to expect negative expansion in zinc oxide at low temperatures, a result which the later experiments of Ibach[18] and the present work have confirmed. This value of γ_0 is important in the present context in that it permits a crude interpolation to complete the temperature dependence of γ at the lowest temperatures. Apart from the fact that γ is negative over a substantial range of temperature, the over-all shape of the curve is similar to that observed earlier in, e.g., alkali halides with the rocksalt structure, and it is tempting to associate the shapes of the $\gamma_{\parallel}$ vs T and $\gamma_{\perp}$ vs T curves, as well as their similarity, with the low degrees of structure anisotropy.

2. *Zinc Sulfide*

Zinc sulfide may commonly exist in two forms, one of which is basically cubic in form, known

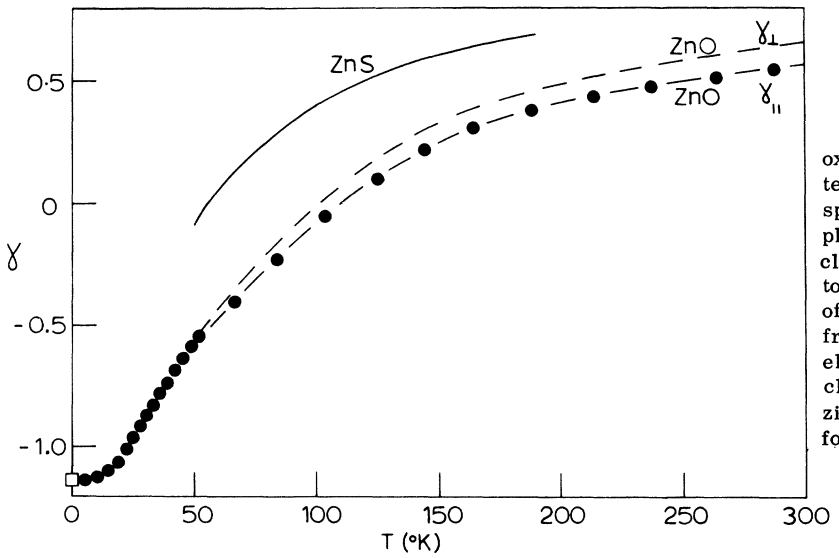

FIG. 3. Grüneisen parameters of zinc oxide and zinc sulfide as functions of temperature. Dashed line: $\gamma_{\perp}$ corresponding to the *a-a* crystallographic-plane direction of zinc oxide; closed circle-dash-closed circle: $\gamma_{\parallel}$ corresponding to the *c* crystallographic-axis direction of zinc oxide; open square: calculated from the pressure dependence of the elastic constants of zinc oxide (Ref. 27); closed circles: isotropic values of γ for zinc oxide, interpolated; solid line: γ for zinc sulfide.

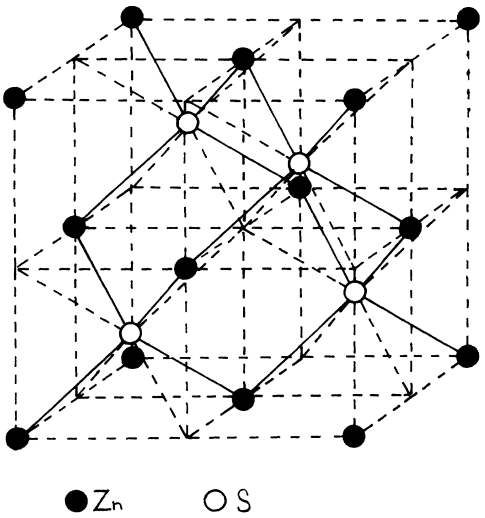

FIG. 4. Sphalerite structure of zinc sulfide.

alternatively as sphalerite, zinc blende, or β zinc sulfide, and the other of which has basically hexagonal symmetry, being commonly known as the wurtzite modification. The subject of the present analysis is the first of these two forms of the solid, which is depicted in Fig. 4. The gram-molecular volume was taken as (23.80 ± 0.05) cm^3 mole^{-1} at room temperature.

Low-temperature specific-heat results due to Martin[30] are available between 4 and 19 °K, which join up reasonably smoothly with the results of Clusius and Harteck,[24] whose data extend between 18 and 197 °K. Alternative earlier data are available[31] in the temperature range 21–59 °K, but these display a rather high degree of scatter and, moreover, they lie above the results of Clusius and Harteck by values up to 20%. The data of Clusius and Harteck were adopted for the present analysis, and it may be noted that no results were available above 197 °K. The difference between extreme values for the thermal expansion of zinc sulfide at room temperature, due to Kopp[32] and Skinner,[33] amounts to some 34%. Data extending to lower temperatures due to Adenstedt[34] and to Reeber and McLachlan[35] lie between these extremes, but disagree between themselves by approximately 40% at 150 °K. No usable results exist below 50 °K, although the trend indicates a change of sign of the volume coefficient of thermal expansion occurring in the vicinity of 55 °K. A compromise was made in adopting low-temperature thermal-expansion data, preference being given to the results of Adenstedt, whose results displayed the lesser scatter, and whose results for lithium fluoride were in good agreement with those of other workers.[36] Extrapolation was employed between 50 and 0 °K. The elastic constants of zinc blende have been measured at room temperature.[37–40] The difference between the extreme values amounts to approximately 7% in c_{11} and approximately 17% in c_{12}. The only results below room temperature are those of Zarembovitch,[40] which extend down to 93 °K, and those of Berlincourt *et al.*,[38] who gave isolated values of c_{11} and c_{12} at 77 °K, which lie above the extrapolated results of Zarembovitch by approximately 1.5 and 2%, respectively. The results of Zarembovitch were extrapolated to $T = 0$ and adopted in the calculations for this material. The Grüneisen parameter was calculated in the usual way, producing the results displayed in Fig. 3. Because of the restricted temperature range over which it was possible to calculate γ, it is difficult to offer many comments on this graph, except to say that it resembles the corresponding curves for zinc oxide both in shape and in the fact that it seems likely to assume negative values at low temperatures.

B. Moments of Frequency Distributions

Before any thermodynamic analysis may be undertaken, it is necessary to calculate the specific heat at constant strain C_η from the experimental values which refer to constant stress C_t. In the case of a solid possessing hexagonal symmetry this may be achieved with the aid of the equation

$$C_t/C_\eta = 1 + T(2\alpha_\perp\gamma_\perp + \alpha_{||}\gamma_{||}) \ . \tag{3}$$

In the case of cubic solids $\alpha_\perp = \alpha_{||}$ and $\gamma_\perp = \gamma_{||}$. C_t and C_η are usually expressed as the quantities referring to constant pressure and volume, respectively, i.e.,

$$C_p/C_v = 1 + 3\alpha\gamma T \ . \tag{4}$$

1. *Zinc Oxide*

The difference between C_t and C_η was calculated at 300 °K from Eq. (3) as $(0.02_8 \pm 0.01_4)$ cal deg^{-1} mole^{-1}. This represents only approximately 0.3% of the measured heat capacity, which is appreciably less than the experimental uncertainty of approximately 4% and which will diminish with reduction of temperature in a manner which cannot be calculated in the absence of elastic-constant data below room temperature. For this reason no correction was applied for $(C_t - C_\eta)$.

As a first step towards calculating the positive even moments, a graph of $[\theta(T, \eta_T)]^2$ was plotted against T^{-2}, and the region lying in the approximate range $\frac{1}{6}\theta < T < \frac{1}{3}\theta$ was extrapolated to $T^{-2} = 0$, in order to gain a first estimate of $\theta(\infty, \eta_0)$. This was substituted in the expression for the dimensionless parameter t defined in the equation

$$t = [1 + (T/0.2\theta_\infty^c)^2]^{-1} \ , \tag{5}$$

in which θ_∞^c is the high-temperature limiting value of the Debye characteristic temperature correspond-

ing to the specific heat.[41] Values of $\gamma_\perp$ and $\gamma_\parallel$ were then plotted against the values of t so obtained, and by extrapolating the graphs to $t=0$, values of $\gamma_\perp$ and $\gamma_\parallel$ corresponding to $T=\infty$ were obtained. In terms of the nomenclature introduced earlier, these two quantities will be referred to as $\gamma_\perp(0)$ and $\gamma_\parallel(0)$. These were applied in place of $\gamma_\perp(2)$ and $\gamma_\parallel(2)$ in the equation

$$\frac{\theta^c(T,\eta_0)}{\theta^c(T,\eta_T)}=\left(\frac{a_T}{a_0}\right)^{2\gamma_\perp(2)}\left(\frac{c_T}{c_0}\right)^{\gamma_\parallel(2)},$$

for which an approximate correction of the Debye temperatures was made to fixed strain corresponding to $T=0$. In effecting this correction, it had been implicitly assumed that values of $\gamma(0)$ and $\gamma(2)$ were very similar. We have defined

$$\frac{a_T}{a_0}=\frac{1-\int_T^{300}\alpha_a dT}{1-\int_0^{300}\alpha_a dT},$$

where

$$\alpha_a=\alpha_\perp=\frac{1}{a_{300}}\frac{da}{dT}$$

and

$$\frac{c_T}{c_0}=\frac{1-\int_T^{300}\alpha_c dT}{1-\int_0^{300}\alpha_c dT},$$

where

$$\alpha_c=\alpha_\parallel=\frac{1}{c_{300}}\frac{dc}{dT}.$$

In evaluating a_T/a_0 and c_T/c_0, the appropriate length changes (in the a and c directions) were estimated at the lowest temperatures, and the calculated correction at room temperature of 0.2% justified this approximation.

A graph of $[\theta^c(T,\eta_0)]^2$ against T^{-2} was then extrapolated to $T^{-2}=0$ from the approximate temperature region $\frac{1}{6}\theta_\infty^c$ to $\frac{1}{3}\theta_\infty^c$, and on the assumption that anharmonic effects had not become unduly serious at $\frac{1}{3}\theta_\infty^c$, "harmonic" heat capacities $C_{\rm har}$ were estimated from the extrapolated region. The point of intersection with the $[\theta^c(T,\eta_0)]^2$ axis at $T^{-2}=0$ yielded a value of $\theta_\infty^c=(706\pm36)$ °K which was used in calculating $\langle\omega^2\rangle$, $\langle\omega^4\rangle$, and $\langle\omega^6\rangle$ using the equations outlined by Barron *et al.*[42] The calculations of the other moments $\langle\omega^n\rangle$ of the frequency distribution $G(\omega)$ defined by

$$\langle\omega^n\rangle=\int_0^\infty\omega^n G(\omega)\,d\omega\Big/\int_0^\infty G(\omega)\,d\omega$$

and the corresponding maximum frequencies of the Debye distributions having the same nth moments as the actual crystal

$$\omega_D(n)=[\tfrac{1}{3}(n+3)\langle\omega^n\rangle]^{1/n}\quad(n\neq0)$$

were calculated for $-3\le n\le6$ using the procedure mentioned earlier,[42] the particularly relevant equations which have been summarized by Bailey and Yates.[43] As explained in these earlier works, the evaluations were effected at the lowest temperatures at which terms beyond those in T^{-6} were negligible in comparison with the rest of the summed quantities.

The calculation of the negative moments calls for special comment. A value of $\theta(0,\eta_0)$ was estimated from the room-temperature elastic constants,[26] neglecting any variation of these quantities between 300 and 0 °K. This was used to derive the value $(12.9\pm1.8)\times10^{-6}$ cal mole^{-1}deg^{-4} for the leading coefficient in the expansion

$$C_v=aT^3+bT^5+cT^7+\cdots$$

from which the very low-temperature heat capacity was estimated. This low-temperature heat capacity was applied to the equation

$$\langle\omega^{1-n}\rangle=\frac{1}{\Gamma(n+1)\zeta(n)}\left(\frac{\hbar}{k}\right)^{n-1}\left[\frac{1}{3Nk}\int_0^T\frac{C_{\rm har}}{T^n}\,dT+\frac{1}{n-1}\frac{1}{T^{n-1}}-\sum_{s=1}^{\infty}(-1)^{s+1}\frac{B_{2s}}{(2s)!}\frac{2s-1}{2s+n-1}\left(\frac{\hbar}{k}\right)^{2s}\frac{\langle\omega^{2s}\rangle}{T^{2s+n-1}}\right]\quad(1<n<4)$$

to estimate $\langle\omega^{-1}\rangle$ and $\langle\omega^{-2}\rangle$. The characteristic temperatures coresponding to the maximum frequencies of the Debye distributions having the same nth moments as the spectrum in the actual crystal were then calculated from $\theta(n)=\hbar\omega_D(n)/k$, except for the following two values of $\theta(n)$ which were given directly as

$$\theta(0)=\frac{\hbar}{k}e^{1/3}\omega_g$$

and

$$\theta(-3)=\theta(0,\eta_0).$$

The results of these calculations are summarized in Table II and Fig. 5.

TABLE II. Values of $\theta(n)$ and $\gamma(n)$ for zinc oxide and zinc blende as a function of order n.

	Zinc oxide			Zinc blende	
n	$\theta(n)$ (°K)	$\gamma_\parallel(n)$	$\gamma_\perp(n)$	$\theta(n)$ (°K)	$\gamma(n)$
−3	416±21	−1.13	−1.13	315±10	
−2	367±20	−0.58±0.04	−0.47±0.04	305±5	
−1	417±14	0.04±0.04	0.13±0.04	336±5	
0	521±17	0.7±0.1	0.8±0.1	381±11	0.8±0.2
2	706±36	1.2±0.2	1.3±0.2	460±14	1.3±0.3
4	812±43	1.3±0.4	1.4±0.4	495±19	1.3±0.9
6	855±41			510±21	

2. *Zinc Sulfide*

Although the difference of the specific heats (C_p-C_v) was only 0.2% at 190 °K in the case of zinc

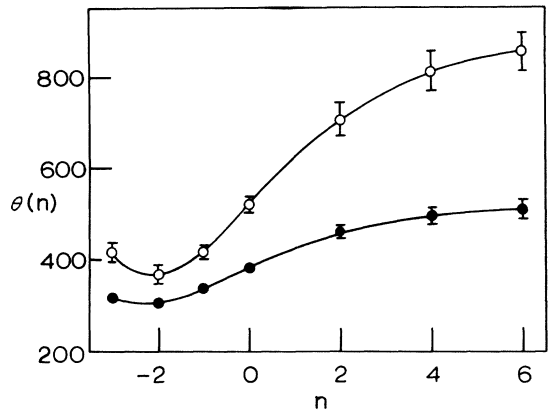

FIG. 5. Function $\theta(n) = \hbar\omega_D(n)/k$ for zinc oxide, ○, and zinc sulfide, ●, in which the uncertainties are indicated by the vertical lines where these exceed the diameters of the circles.

sulfide, i.e., smaller than the experimental uncertainty, it was applied, nevertheless, since sufficient data were available to permit its estimation over the greater part of the temperature range of the analysis. The calculation of the even positive moments followed the procedure described for ZnO, except that the graph of

$$\{1-[\theta^c(V_0)/\theta^c_\infty(V_0)]^2\}[\theta^c_\infty(V_0)/T]^{-2}$$

against $[\theta^c_\infty(V_0)/T]^2$ proved to be particularly sensitive to the value taken for $\theta^c_\infty(V_0)$ above $T \approx \frac{1}{5}\theta^c_\infty$. The curves below this temperature behaved in a much more consistent fashion, and for this reason calculations of $\omega_D(4)$ and $\omega_D(6)$ were based upon the approximate temperature range $\frac{1}{5}\theta^c_\infty$–$\frac{1}{9}\theta^c_\infty$ and a value of $\theta^c_\infty(V_0) = (460 \pm 14)$ °K which was calculated in the usual way. The ω_g was calculated in the manner described earlier, after first calculating the "harmonic" entropy. The value of θ_0 was taken from the low-temperature specific-heat results,[30] and the experimental uncertainty was assessed from the author's graph, leading to a value of $\theta_0 = 315 \pm 10$ °K. The $\langle\omega^{-1}\rangle$ and $\langle\omega^{-2}\rangle$ were calculated in the straightforward way which has also been described earlier. The absence of any peculiarities in the values of $\theta(n)$ which resulted from these calculations was taken as justification for the determination of $\theta(1)$, required for the later calculation of the zero-point energy, by interpolation.

C. Volume Dependence of Moments

The influence of volume upon the characteristic temperatures corresponding to the entropy, heat capacity, and Debye-Waller frequency integral may all be calculated with the aid of the volume dependence of the moments,[41] conveniently expressed in terms of the parameter

$$\gamma(n) = \sum_{j=1}^{3N-6} \gamma_j \omega_j^n \Big/ \sum_{j=1}^{3N-6} \omega_j^n = -\frac{d\ln\omega_D(n)}{d\ln V} = -\frac{1}{n}\frac{d\ln\langle\omega^n\rangle}{d\ln V} .$$

1. *Zinc Oxide*

Pursuing the consequences of the quasiharmonic approximation, the volume dependences of the positive even moments $\gamma_\parallel(2)$, $\gamma_\perp(2)$, $\gamma_\parallel(4)$, and $\gamma_\perp(4)$ were determined from the intercept and the first differential coefficient of the high-temperature expansion given by Barron *et al.*[41] in the rearranged form

$$(\gamma_\infty - \gamma)T^2 = \frac{\langle\omega^2\rangle}{12}\left(\frac{\hbar}{k}\right)^2[\gamma(2)-\gamma(0)] - \frac{1}{T^2}\left(\frac{\hbar}{k}\right)^4\left\{\frac{\langle\omega^4\rangle}{240}[\gamma(4)-\gamma(0)] - \left(\frac{\langle\omega^2\rangle}{12}\right)^2[\gamma(2)-\gamma(0)]\right\}$$
$$+ \frac{1}{T^4}\left(\frac{\hbar}{k}\right)^6\left\{\frac{\langle\omega^6\rangle}{6048}[\gamma(6)-\gamma(0)] - \frac{\langle\omega^2\rangle}{12}\frac{\langle\omega^4\rangle}{240}[\gamma(4)-\gamma(0)] + \frac{\langle\omega^2\rangle}{12}\left[\left(\frac{\langle\omega^2\rangle}{12}\right)^2 - \frac{\langle\omega^4\rangle}{240}\right][\gamma(2)-\gamma(0)]\right\} - \cdots .$$

The experimental uncertainties become prohibitively large with increasing n. This was the reason for not carrying the calculations beyond the determinations of $\gamma_\parallel(4)$ and $\gamma_\perp(4)$. Values of $\gamma_\parallel(0)$ and $\gamma_\perp(0)$ were given by the values of γ_λ^∞ calculated earlier. In determining $\gamma_\parallel(-1)$ and $\gamma_\perp(-1)$ from the equation

$$\gamma(n) = \int_0^\infty \gamma C_{\rm har}\, T^{n-1} dT \Big/ \int_0^\infty C_{\rm har}\, T^{n-1}\, dT \qquad (-3 < n < 0) , \quad (6)$$

the evaluations were performed at a series of finite temperatures. The resulting approximations to $\gamma_\parallel(-1)$ and $\gamma_\perp(-1)$ were plotted against T^{-1} and extrapolated to $T^{-1} = 0$ to give the values which were finally adopted. The results of the calculations are summarized in Table II and displayed graphically in Fig. 6, in which $\gamma(-3) \equiv \gamma_0$ was the value corresponding to the pressure dependence of the elastic constants mentioned earlier.[27] Figure 6 shows the mean values of $\gamma_\parallel(n)$ and $\gamma_\perp(n)$, where these may be compared with the corresponding result for zinc sulfide.

2. *Zinc Sulfide*

In attempting to calculate the volume dependences of the positive even moments, the procedure de-

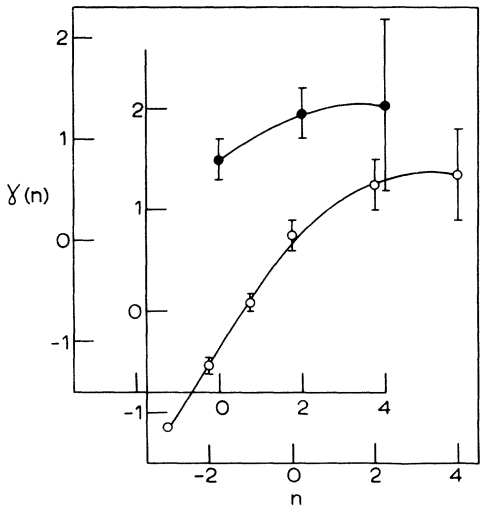

FIG. 6. Variation of the volume dependences of the moments $\gamma(n)$ with n for zinc oxide, O, and zinc sulfide, ●, in which mean values for the c and a crystallographic-axis directions have been plotted for zinc oxide, and the uncertainties are indicated by the vertical lines.

scribed for zinc oxide was again used, except that attention was concentrated on the approximate temperature region $\frac{1}{9}\theta_\infty^c < T < \frac{1}{5}\theta_\infty^c$ instead of the more usual range $\frac{1}{6}\theta_\infty^c < T < \frac{1}{3}\theta_\infty^c$ for the reason described earlier. Because of experimental uncertainties at the higher temperatures, it was not possible to extend calculations of $\gamma(n)$ beyond $n=4$. The $\gamma(0)$ was given by γ_∞ as before, and a serious attempt was made to evaluate $\gamma(-1)$ using Eq. (6). However, it turned out that the value of the numerator of the right-hand side of this expression between $T=0$ and 50 °K was likely to be anything up to 100% of the corresponding value of the integral between 50 and 190 °K. Even with good thermal-expansion and elasticity data below 50 °K, the extrapolation of the ratio used to determine $\gamma(-1)$ from the highest temperature at which specific-heat results exist (190 °K, up to $T=\infty$) would introduce uncertainties. Without any thermal-expansion results below 50 °K, estimates would be so crude as to be valueless. Similar remarks apply to the case of $\gamma(-2)$, except that here the situation is even more serious. Finally, it is quite impossible to estimate $\gamma(-3)$ by extrapolating the γ data from $T=50$ °K to $T=0$, and unfortunately there are no experimental data concerning the pressure dependences of the elastic constants, from which $\gamma(-3)\equiv\gamma_0$ could be calculated. The results of the calculations of the moments and their volume variations are summarized in Table II and displayed in Figs. 5 and 6.

D. Amplitudes of Vibration

Starting with a result deduced by Blackman[13] on the basis of assumed harmonic lattice vibrations, Leadbetter[44] has used the Debye-Waller frequency integral $X(T)$ discussed earlier[45] to derive expressions for the mean square amplitudes of the atoms and molecules of ice. Adapting these expressions to the present situation, the mean mass m and the mean square amplitude of vibration $\bar{u}^2$ of the atoms in the II-VI compounds are related to $X(T)$ through

$$m\bar{u}^2 = X(T) \ . \tag{7}$$

In the low-temperature limit $X(T)=\frac{1}{2}\hbar\langle\omega^{-1}\rangle$, whereas for $T>\theta_\infty^c/2\pi$

$$X(T) = kT\left[\langle\omega^{-2}\rangle + \frac{1}{12}\left(\frac{\hbar}{kT}\right)^2 - \frac{1}{720}\left(\frac{\hbar}{kT}\right)^4\langle\omega^2\rangle - \cdots\right] \ . \tag{8}$$

On the basis of Eqs. (7) and (8), the rms amplitudes of vibration of the atoms $(\bar{u}^2)^{1/2}$ have been calculated. These are displayed graphically in Fig. 7. The results are believed to be correct to within a few percent, and to agree well with calculations based upon simple shell models. In particular, in the case of zinc sulfide the rms amplitude of vibration based upon the present calculations is lower than that calculated on the basis of the shell model of Hewat[12] by only approximately 6% at 0 °K, and higher by only approximately 2% at 300 °K. Similar figures apply in the case of zinc oxide.[12,46]

IV. CONCLUSIONS

Considering the characteristic temperatures cor-

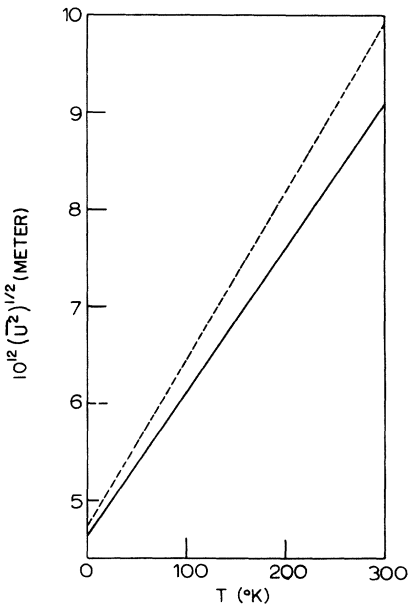

FIG. 7. The rms amplitudes of vibration of the atoms $(\bar{u}^2)^{1/2}$ in zinc oxide (solid line) and zinc sulfide (dashed line).

responding to the cutoff frequencies of the Debye distributions having the same nth moments as the frequency spectra in the actual cyrstals, depicted in Fig. 5, certain observations are possible. The spread in values of $\theta(n)$ in the range $-2 \leq n \leq 6$ is considerably greater for zinc oxide and zinc sulfide than is the case with simple ionic solids.[17,43,47] This is particularly so in the case of zinc oxide. Also the ratio $\theta(6)/\theta(-2)$ is high compared with the corresponding values for other solids, and again the difference is particularly marked in the case of zinc oxide. The approximate value of this ratio for zinc ozide is 2.3, and for zinc sulfide 1.7. Zinc, which also possesses hexagonal symmetry, has a value of 1.4, the simple ionic solids have values ranging between 1.4 and 1.2, and the values for germanium and silicon are found around 1.2 or 1.1. These last named substances, having low values for the ratio $\theta(6)/\theta(-2)$, all have one factor in common: They have cubic symmetry. Remarks similar to those for zinc oxide may also be made about pyrolytic graphite,[48] which also has hexagonal symmetry but which is very anisotropic. The above figures suggest that the vibrational spectra in zinc oxide and sphalerite zinc sulfide are more complex than in a number of other solids, particularly than in those other solids having cubic symmetry. This indicated complexity is not difficult to understand. Zinc oxide, zinc, and pyrolytic graphite all have hexagonal symmetry, and to this extent thay are structurally more complex than cubic solids. This feature alone might be expected to lead to complex spectra. In the case of zinc, however, the atoms are all of the same type, which might be expected to lead to a simpler situation than that in zinc oxide, in which there are two different atoms.

Turning to the volume dependence of the frequencies, the striking feature of Fig. 3 is the similarity of the values of $\gamma_{\parallel}$ and $\gamma_{\perp}$ for zinc oxide, which supports the conclusion that the vibrations parallel and perpendicular to the c crystallographic axis in zinc oxide must be basically very similar. Examinations of the wurzite structure bear out a similarity of the form and dimensions of the crystal structure in these two mutually perpendicular directions. The mean values of $\gamma(n)$ for values of $n \sim 4$ or higher are dominated by the high-frequency modes, and the fact that $\gamma(n)$ is positive for positive n suggests that these modes may be predominantly longitudinal. It may be inferred that the forces between the atoms are comparatively strong and that the complete vibrational frequency spectrum contains a considerable proportion of high-frequency modes. In the case of zinc oxide, the $\gamma_{\lambda}(n)$ become quite markedly negative as n becomes increasingly negative, implying the preponderance of transverse modes of vibration over the longitudinal contribution among the low frequencies.

Finally, attempting to get some indication about the magnitude and nature of anharmonic effects in these solids, after calculating the zero-point energy E_z of the crystals, the ratios of the thermal energies at $T \approx \frac{1}{3}\theta_{\infty}^{c}$ to E_z were evaluated. The ratios turned out to be very similar to the corresponding figures for simple ionic solids. Looking next at the ratios of the amplitudes of vibration at 300 °K to the interatomic spacing, we find again that the figures turn out to be very similar to those for simple ionic solids. On the other hand, the thermal expansions are very much smaller indeed than values for simple ionic solids at the same reduced temperatures. It is possible that these observations may add up to an indication of the existence of an unusually large constant-volume explicitly temperature-dependent contribution to the anharmonicity at an unusually low reduced temperature.

In may be shown that the anharmonic contribution to the heat capacity may be represented by

$$\Delta C^{\mathrm{anh}} = BE_T \sum_j \left(\frac{\partial C_j^{\mathrm{har}}}{\partial \ln \nu_j}\right)_T - B(C^{\mathrm{har}})^2 T ,$$

in which E_T is the thermal energy and the shift in the normal-mode frequency ν_j has been written as

$$\delta\nu_j/\nu_j = B_j(E_z + E_T)$$

and all the values of B_j have been assumed to be constant for any particular crystal. In this expression, C_j^{har} is the contribution to the harmonic heat capacity from the jth normal mode. B may be estimated by a reiterative procedure when precise experimental data exist. Attempts have been made to calculate a first approximation to B for zinc oxide, giving a value which is higher than those for alakali halides by a factor of approximately 10, but which is of a similar order to values observed for solid argon and ice. From a more precise value of B, the volume-dependent shift of the geometric mean frequency could be calculated, which must be related to corresponding temperature-dependent shifts in the infrared absorption and neutron scattering properties of the crystals. The experimental data permitting such comparisons would be extremely valuable.

ACKNOWLEDGMENTS

We wish to express our gratitude to the Aerospace Research Laboratories, WPAFB, Ohio, for the specimens of zinc oxide. We are also grateful to B. W. James, University of Salford, for estimating $\theta(-3)$ for zinc oxide using calculations based upon the room-temperature elastic constants. Thanks are also due to Dr. R. R. Reeber, Michigan State University, for access to his unpublished data for zinc oxide, and to Dr. A. W. Hewat, University of Melbourne, for the results of his shell-model calculations of vibrational amplitudes in sphalerite

zinc sulfide prior to publication. B. Y. wishes to record his gratitude to the University of Dayton and to the U. S. Air Force for an engagement at the Aerospace Research Laboratories. R. F. C. wishes to record his gratitude to the British Oxygen Co. Ltd., for financial support.

---

*Sponsored in part or in whole by the Aerospace Research Laboratories, Office of Aerospace Research, United States Air Force, Contract No. F33615-67-C-1027.

†Research carried out with financial support from the British Oxygen Co. Ltd.

[1]*Proceedings of the International Conference on II-VI Semiconducting Compounds*, edited by D. G. Thomas (Benjamin, New York, 1968).

[2]*Physics and Chemistry of II-VI Compounds*, edited by M. Aven and J. S. Prener (Wiley, New York, 1967).

[3]D. C. Reynolds, C. W. Litton, and T. C. Collins, Phys. Status Solidi 9, 645 (1965); 12, 3 (1965).

[4]G. Heiland and H. Ibach, Solid State Commun. 4, 353 (1966).

[5]T. C. Damen, S. P. S. Porto, and B. Tell, Phys. Rev. 142, 570 (1966).

[6]G. D. Archard, Acta Cryst. 6, 657 (1953).

[7]D. H. Chung and W. R. Buessem, J. Appl. Phys. 39, 2777 (1968).

[8]A. K. Rajagopal and R. Srinivasan, Z. Physik 158, 471 (1960). It has been pointed out that the calculation is in error because a first-order term is forgotten.

[9]S. J. Czyzak, J. C. Manthuruthil, and D. C. Reynolds, J. Appl. Phys. 33, 180 (1962).

[10]A. J. Majumdar and R. Roy, Am. Mineralogist 50, 1121 (1965).

[11]R. W. Keyes, J. Appl. Phys. 33, 3371 (1962).

[12]A. W. Hewat (unpublished).

[13]M. Blackman, Acta Cryst. 9, 734 (1956).

[14]N. Waterhouse and B. Yates, Cryogenics 8, 267 (1968).

[15]R. F. Cooper and B. Yates, J. Phys. C 3, L12 (1970); M. Gluyas, F. D. Hughes, and B. W. James, J. Phys. E 3, 132 (1970).

[16]B. W. James and B. Yates, Cryogenics 5, 68 (1965).

[17]A. C. Bailey and B. Yates, Phil. Mag. 16, 1241 (1967).

[18]H. Ibach, Phys. Status Solidi 33, 257 (1969).

[19]A. A. Khan, Acta Cryst. A24, 403 (1968).

[20]D. B. Sirdeshmukh and V. T. Deshpande, Current Sci. (India) 36, 630 (1967).

[21]R. R. Reeber (unpublished).

[22]T. H. K. Barron and R. W. Munn, Phil. Mag. 15, 85 (1967).

[23]C. G. Maier, G. S. Parks, and C. T. Anderson, J. Am. Chem. Soc. 48, 2564 (1926).

[24]K. Clusius and P. Harteck, Z. Physik. Chem. 134, 243 (1928).

[25]V. Tarnow, J. Phys. D 2, 1383 (1969).

[26]T. B. Bateman, J. Appl. Phys. 33, 3309 (1962).

[27]N. Soga and O. L. Anderson, J. Appl. Phys. 38, 2985 (1967).

[28]T. H. K. Barron, Phil. Mag. 46, 720 (1955).

[29]D. E. Schuele and C. S. Smith, J. Phys. Chem. Solids 25, 801 (1964).

[30]D. L. Martin, Phil. Mag. 46, 751 (1955).

[31]P. Gunther, Ann. Physik 51, 828 (1916).

[32]H. Kopp, Ann. Chem. Pharm. 81, 1 (1852).

[33]B. J. Skinner, Mineral., Geochem., and Petrol. Art. 152, D109 (1962).

[34]H. Adenstedt, Ann. Physik 26, 69 (1936).

[35]R. R. Reeber and D. McLachlan, Defense Documentation Center, Cameron Station, Alexandria, Va. 22314, USAF Report ARL-68-0183 (unpublished).

[36]B. Yates and C. H. Panter, Proc. Phys. Soc. (London) 80, 373 (1962).

[37]B. H. Krishna Murty and B. Subrahmanyam, J. Sci. Indust. Res. 20B, 448 (1961).

[38]D. Berlincourt, H. Jaffe, and L. R. Shiozawa, Phys. Rev. 129, 1009 (1963).

[39]N. G. Einspruch and R. J. Manning, J. Acoust. Soc. Am. 35, 215 (1963).

[40]A. Zarembovitch, J. Phys. (Paris) 24, 1097 (1963).

[41]T. H. K. Barron, A. J. Leadbetter, and J. A. Morrison, Proc. Roy. Soc. (London) A279, 62 (1964).

[42]T. H. K. Barron, W. T. Berg, and J. A. Morrison, Proc. Roy. Soc. (London) A242, 478 (1957).

[43]A. C. Bailey and B. Yates, Proc. Phys. Soc. (London) 91, 390 (1967).

[44]A. J. Leadbetter, Proc. Roy. Soc. (London) A287, 403 (1965).

[45]T. H. K. Barron, A. J. Leadbetter, J. A. Morrison, and L. S. Salter, *Inelastic Scattering of Neutrons in Solids and Liquids* (International Atomic Energy Agency, Vienna, 1963), Vol. 1, p. 49.

[46]A. W. Hewat, Solid State Commun. 8, 187 (1970).

[47]A. J. Kirkham and B. Yates, J. Phys. C 1, 1162 (1968).

[48]A. C. Bailey and B. Yates, UKAEA TRG Report No. 1874 (C/X), 1969 (unpublished).